

Temperature Distribution and Weld Bead Geometry Analysis in MIG Welded AA6061 Alloy using Finite Element Analysis

Vinoth A¹, Sivasankari R¹, Krishnamoorthi J¹

1-PSG College of Technology, Coimbatore, Tamil Nadu, India

ABSTRACT

In the present work, FEA (Finite Element Analysis) of chosen Aluminum alloy MIG welding was carried out to perform thermal distribution analysis and weld bead geometry prediction. A double ellipsoidal heat source model was designed and the thermal analysis was carried out for the chosen AA6061 Aluminum alloy process parameters using the Heat Source Fitting (HSF) tool module in Sysweld 15.0 simulation software. The simulated weld bead dimensions display good agreement with the actual weld bead dimensions with 90% accuracy. Thus, with the modeled heat source the optimization of the process parameters for obtaining the required bead geometry was attainable with minimal weld trials.

Key words: Aluminum Alloy, MIG Welding, Finite Element Analysis.

I. Introduction

Aluminum alloy AA6061 is a combination of aluminum, silicon, and magnesium alloys. This alloy is commonly used for a wide range of products, including automotive parts, airplanes and aerospace supplies, marine industries, and so on. AA6061 has high hardness, corrosion resistance and wear resistance as well as good welding and fatigue resistance [1]. A major progress in the production of aluminum and its alloys came about with the development of the MIG and TIG welding processes. These arc welding processes made a high strength weld without the need for aggressive fluxes [2]. To obtain a good quality weld and subsequently increase the productivity of the process, it is therefore, necessary to control the welding process parameters. The welding parameters are normally selected based on the experience. This selection procedure does not lead to the optimal and economical use of the machinery and good quality of the surface [3]. Therefore, in order to save time and cost of experiments, the numerical techniques can be employed to simulate welding process and optimize welding parameters.

Finite Element Method (FEM) is very useful for predicting thermal distribution and residual stresses in welded plates [4]. The modeling of moving heat source is an important concern in numerical simulation studies of various welding processes. Gaussian and Double Ellipsoidal Heat Source (DEHS) models were generally used to simulate arc welding processes [5-7]. Francis et. al [8] simulated the welding process for butt and T-joints for 2000 series aluminum alloys using Gaussian heat

source model with finite element method and compared the results with previous experimental data. The results showed that, Gaussian heat source model could not exactly predict the temperature distributions. Bradac et al [9] calibrated the heat source parameters for Gaussian and Double Ellipsoidal models after comparison between numerical results and experimental data. The results revealed that, the prediction of thermal profiles using Double Ellipsoidal heat source model has reasonable agreement with experimental data than the Gaussian heat source model. Ismail et al [10] simulated the MIG welding process by the nonlinear finite element method and investigated the effect of the changing of the voltage and welding speed on the heat distribution in the transition state using Gaussian heat source model. Comparing the temperature distribution and the geometry of weld with the experimental data showed that the change in voltage and welding speed had a significant effect on the distribution of the temperature, and the shape and size of the fillet bead of weld. Argas Javier et al [11] simulated the welding of aluminum alloy 6061-T6 plate with a MIG welding process by finite element method and compared the calculated temperature with the experimental data. Baharnezhad And Golhin [12] examined the effect of crucial parameters on thermal, mechanical, and microstructural behaviors in the MIG welding process of Al6063 by simulation and experiment. The thermo-mechanical model was simulated by Abaqus software, and the temperature distribution and residual stress were obtained. Then, the simulation results were compared with the

experimental data. The results showed that the simulation could exactly predict the temperature and stress distributions.

Several researchers have been done to study the weld thermal analysis of Aluminum alloys using Gaussian heat source model, but very limited researchers were reported the welding simulation using Double Ellipsoidal heat source model. In this work, the numerical MIG welding simulation of Aluminum alloy was carried out using Double Ellipsoidal heat source model and the welding parameters were optimized to achieve the full depth of penetration.

II. EXPERIMENTAL METHODS

2.1 Material and welding

Aluminum alloy AA6061 plates of size 100 mm length, 50 mm width, and 6 mm thickness were used for the preparation of weld joints. The chemical composition of the AA6061 plate is given in table 1. Conventional V-groove butt joint configuration and its dimensions as shown in figure 1 was adopted for the MIG welding with four different heat inputs. Welding conditions and set-up followed during the welding of plates are shown in figure 2. The welding parameters for all the weld coupons are given in table 2.

Table 1. Chemical composition of AA 6061 alloy

Elements	Si	Mg	Cu	Mn	Fe	Al
Wt. %	0.561	0.986	0.31	0.052	0.289	Balance

Table 2. Welding parameters of MIG welding of Al6061

Trial No	Current (Amps)	Voltage (Volts)	Travel Speed (mm/min)	Heat Input (J/mm)
1	160	20.2	400	412
2	160	20.2	380	434
3	160	20.2	350	460
4	160	20.2	300	517

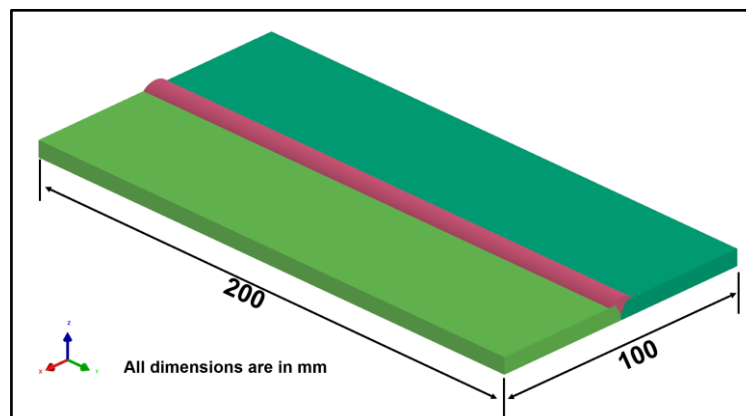


Figure 1. Butt joint configuration of MIG welding of Al6061

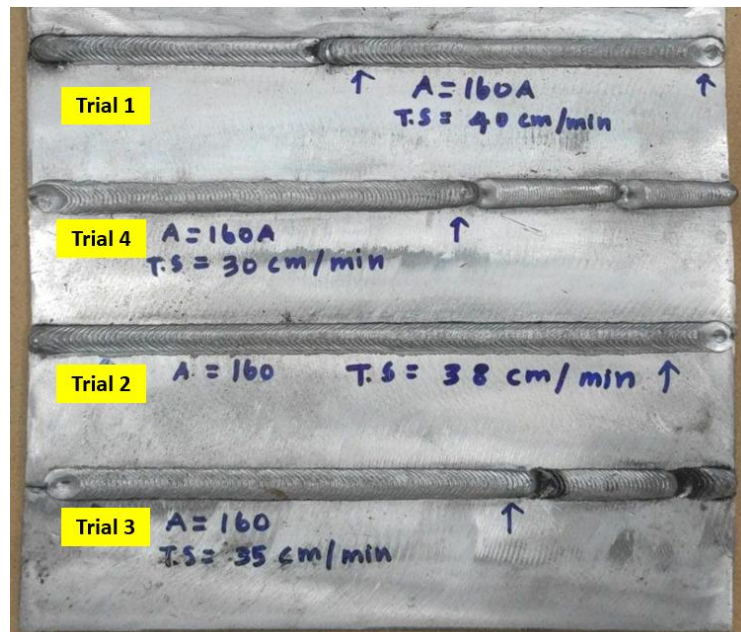


Figure 2. MIG welding trials of Al6061

To investigate fusion zone geometry of the welded joint with four different heat input, a specimen containing the weld metal, HAZ and base metal was cut from all the weld coupons by wire electrical discharge machining process. Then, the surface of the specimens was treated sequentially by mechanical polishing and chemical etching methods as per ASTM E 3 [13]. Killers' reagent was used to evaluate the fusion zone geometry of the weldments using ZEISS Stemi 508 stereo microscopy. The shape and size of the weldment was measured by ZEISS image analysis software.

2.2 Numerical Methods

2.2.1 Finite Element Analysis

Numerical welding simulation is a coupled problem involving thermal and mechanical analysis. It involves heating and cooling of the material which leads to change in phases and material properties

with variation in temperatures[14-15]. In this study, Weld plate was modeled and simulated based on 3D finite element method (FEM) using the Sysweld software. The nonlinear transient heat transfer analysis was performed to determine the temperature distribution and shape and size of the weldment.

2.2.2 Finite Element Model

A 3D finite element analysis was carried out for the weld joint having the dimensions of 200 X 100 X 6 mm using Visual Mesh Software. Fine mesh of size 0.5 X 0.5mm was used for the fusion zone and heat affected zone to capture thermal gradients and fusion zone geometry. A coarse mesh of size 2 X 2mm was used away from the weld to reduce computational time. The figure3 shows the FE mesh for weld, HAZ and away from the weld. Eight node liner heat transfer elements were used in the thermal analysis.

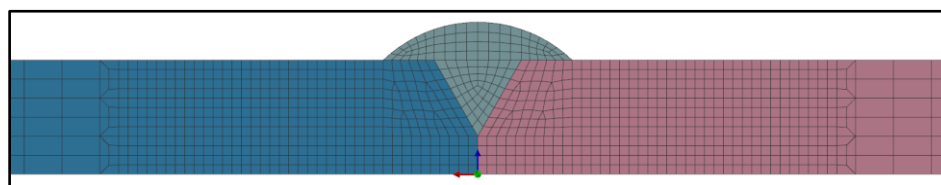


Figure3. FE mesh model

During FE meshing, three types of elements are used (they are one dimensional linear element, 2-D quadrilateral element and 3-D brick element). The one-dimensional linear elements are considered to represent the weld reference and trajectory lines for the weld pass. 2-D Four node

quadrilateral elements are considered to mesh the component surfaces which are subjected to convective and radiative heat losses. 3-D Eight node linear isoparametric brick elements are considered to mesh the weld bead and the base

metal. The figure4 shows 3-D FE mesh model of butt joint configuration used for this analysis.

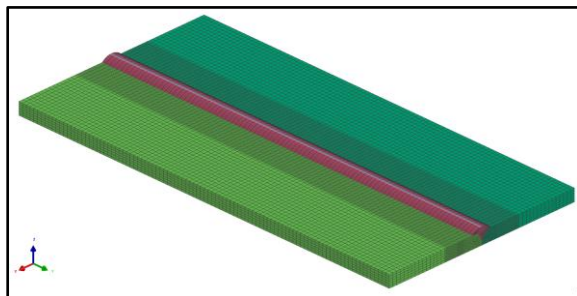


Figure4. 3-D FE mesh model

During welding, a non-uniform temperature field is generated. An accurate thermal analysis with appropriate boundary condition is of paramount importance for the determination of realistic temperature profile to simulate the process. Heat transfer in welding is mainly by conduction and loss to surrounding by convection and radiation. The heat diffusion by conduction is formulated based on the Fourier law [16], where heat flux q (W/m^2) flows from hot to cooler region and is linearly dependent on the temperature gradient. The governing equation 1 of the non-linear transient heat conduction is given by the equation 1.

2.2.3 Thermal analysis

$$Q_v + \left(k(T) \left(\frac{\partial^2 T}{\partial x^2} + \frac{\partial^2 T}{\partial y^2} + \frac{\partial^2 T}{\partial z^2} \right) \right) = \rho(T) c_p(T) \left(\frac{\partial^2 T}{\partial t} \right) \quad \rightarrow 1$$

Where,

Q_v – Volumetric heat flux in $W.m^{-3}$

T – temperature in $^{\circ}C$

$k(T)$ – Thermal conductivity as a function of temperature in $W.m^{-1}k^{-1}$

$c_p(T)$ – Specific heat as a function of temperature in $W.m^{-1}k^{-1}$

$\rho(T)$ – Density as a function of temperature in $Kg.m^{-3}$

(x, y, z) – Space coordinates

t – Time in sec

The temperature dependent Thermo-Physical properties of Al6061 such as density, specific heat capacity, thermal conductivity, and thermal strain was considered for the thermal analysis, and it is shown in the figure5.

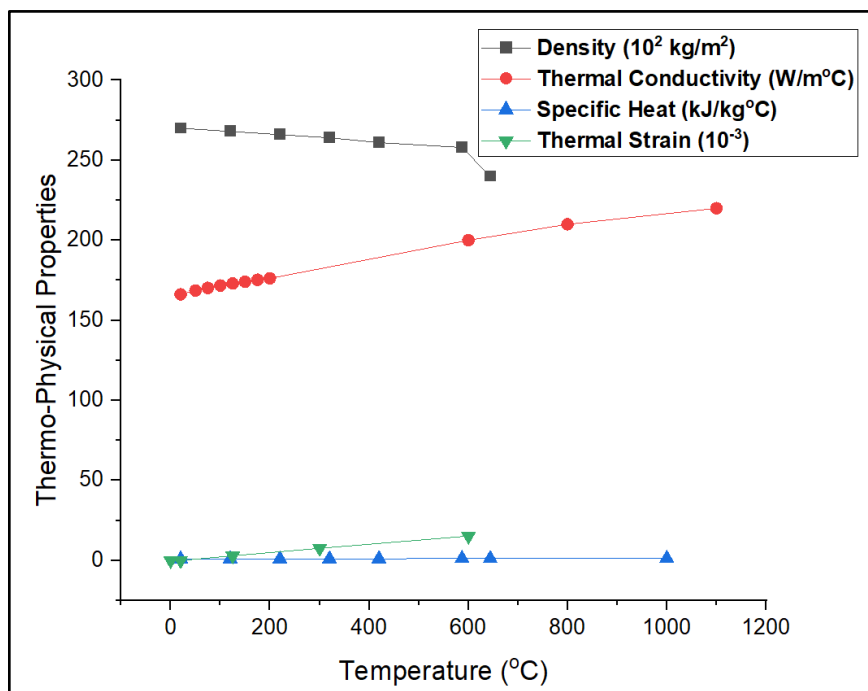


Figure5. Thermo-Physical properties of Al6061

The simulation of welding requires modelling of a heat source and its parameters for activation and deactivation of the deposited weld bead elements. It influences the amount of weld metal melted and defines the weld dimensions. Double Ellipsoidal Heat Source Model (DEHSM) proposed by Goldak et al. [17-18] was used to

simulate volumetric heat deposition during MIG welding. The ellipsoidal heat source is represented by two quadrants i.e., front, and rear halves. Power density distribution (q) inside the front and rear quadrant of the heat source are given in equations 2 and 3, respectively.

$$q_f(x, y, z) = \frac{6\sqrt{3} f_f Q}{a_f b c \pi \sqrt{\pi}} e^{-\frac{3x^2}{a_f^2}} \cdot e^{-\frac{3y^2}{b^2}} \cdot e^{-\frac{3|z+v(\tau-t)|^2}{c^2}} \quad \rightarrow 2$$

$$q_r(x, y, z) = \frac{6\sqrt{3} f_r Q}{a_r b c \pi \sqrt{\pi}} e^{-\frac{3x^2}{a_r^2}} \cdot e^{-\frac{3y^2}{b^2}} \cdot e^{-\frac{3|z+v(\tau-t)|^2}{c^2}} \quad \rightarrow 3$$

Where, $Q = \eta V I$ is the total heat source power [W], a_f, a_r, b, c are the ellipsoidal heat source parameters [m], a_f is front length of molten pool, a_r is rear length of molten pool, c is depth of penetration and b is half width. f_f and f_r are proportional coefficient at front and rear ellipsoid of the heat source respectively, such that $f_f + f_r = 2$, and v is the welding speed [m/s].

The transient type of heat transfer analysis was employed on the DEHSM by varying the four different heat input to achieve the single sided full penetration weld. During the movement of the heat source, the heat energy was kept as constant, but the

location of the center of the heat source changes as a function of time. Using the designed heat source model, MIG welding simulation was carried out and optimized weld parameters were determined.

2.2.4 Boundary conditions

The heat from the deposited material by the heat source is conducted within the plate. At the time of cooling heat is transferred from the plate surface to the surrounding air through convection and radiation [19-20]. The convection (q_{conv}) was calculated using Newton's law.

$$q_{conv} = -h_{conv}(T_s - T_\infty) \quad \rightarrow 4$$

Where, h_{conv} is the heat transfer coefficient, T_s is the surface temperature of the plate and T_∞ is the surrounding temperature which is assumed to be 20 °C. In addition, radiation was modeled using Stefan-Boltzmann law.

$$q_{rad} = -\sigma_{sb} \epsilon_o (T_s^4 - T_\infty^4) \quad \rightarrow 5$$

Where, σ_{sb} is the Stefan-Boltzmann constant which equals $5.672 \times 10^{-8} \text{ W m}^2 \text{ K}^4$.

The surface and skin elements were used to model the convective and radiative heat transfer through the outer surface of the FE model.

III. RESULTS AND DISCUSSION

3.1 Thermal analysis

The numerical simulation is carried out to predict the temperature distribution during welding of Aluminum alloy AA6061 with different heat inputs. The figure 6 shows the isotherms on the outer surface of the MIG welded Aluminum alloy,

AA6061 with different heat inputs at time $t=16.45\text{s}$. It can be seen from the figure; the geometrical characteristic of the weld pool and its temperature distribution is in elliptical shape. The temperature gradient around the weld is evident that the maximum temperature is observed at the center of the weld. At the same time, the closer it is to the maximum temperature area, the denser is the isotherm distribution and the greater is the temperature gradient. On the contrary, in the low-temperature area, the smaller temperature gradient comes with the lower isothermal distribution.

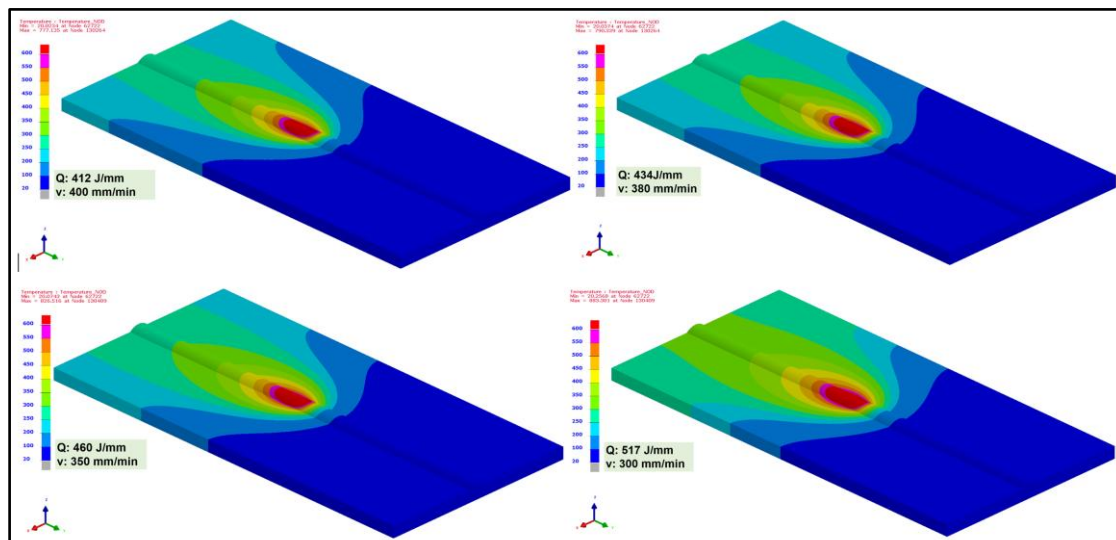


Figure 6. Transient temperature distribution of MIG welding of Al6061

Figure 7 shows the temperature field distribution obtained for welding with parameters of heat input 412 J/mm and 400 mm/min speed. It is observed that the temperature (777 °C) at the fusion zone on the top surface of the plate is high and

temperature (573 °C) is low on the bottom surface of the plate. The result is shown for welding time of 14.50 s. The gradient of temperature becomes insignificant due to insufficient heat energy supplied, that is, 412 J/mm.

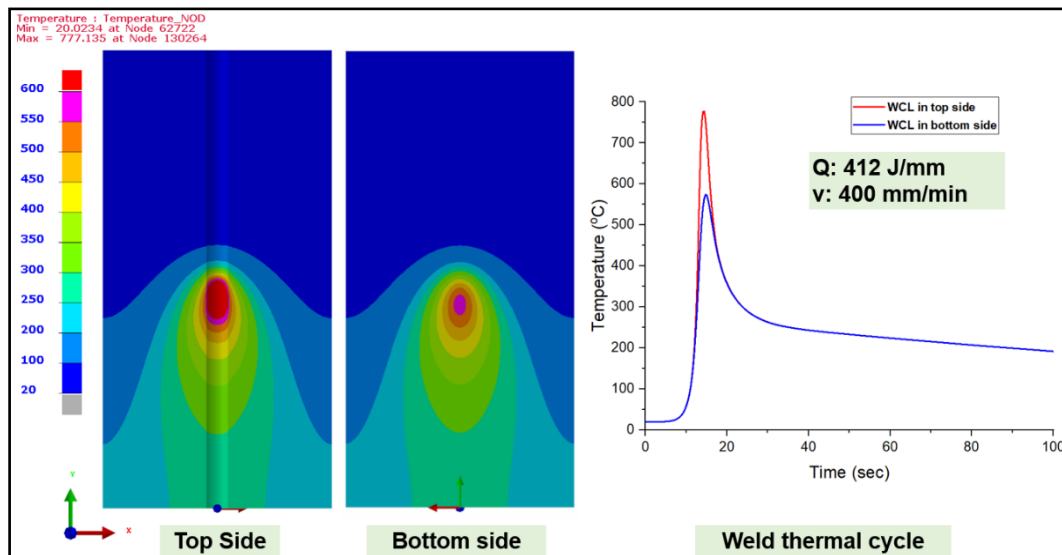


Figure 7. Temperature distribution on the surface for the heat input of 412 J/mm

When the speed of welding is decreased to 350 mm/mm, the supply of heat energy for welding increases from 412 to 350 J/mm. This temperature field distribution is shown in figure 8. It is observed that the temperature (826 °C) at the fusion zone on

the top surface of the plate is high and temperature (585 °C) is low on the bottom surface of the plate. The temperature gradient is slightly increased than the previous condition but there is no evidence of melting of metal at the bottom surface.

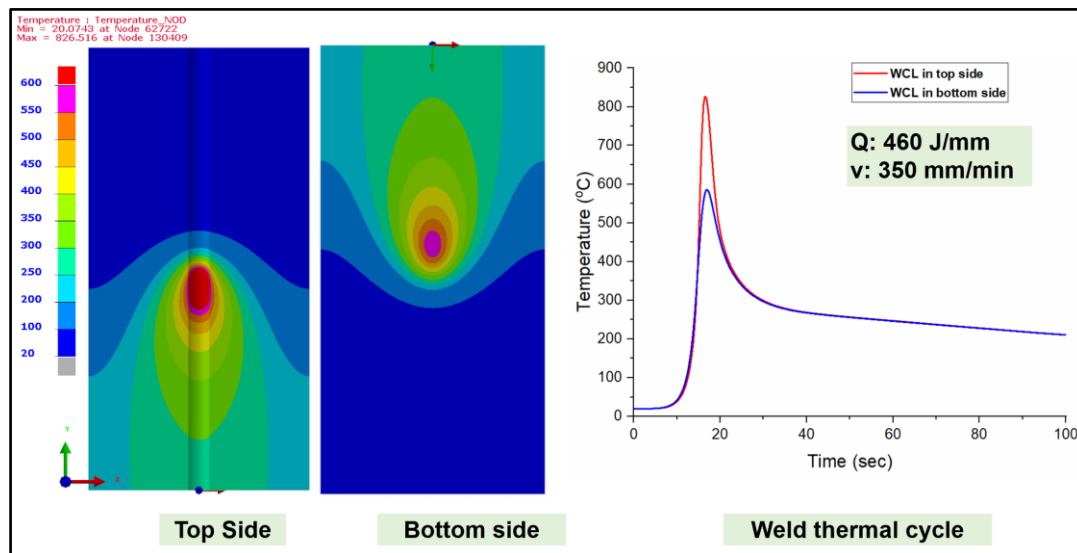


Figure 8. Temperature distribution on the surface for the heat input of 460 J/mm

Figure 9 shows the temperature field distribution of the plate with parameters of 417 J/mm and 300 mm/min speed. The peak temperature rises to 883 °C because more amount of heat energy

is supplied when arc travels with a speed of 300 mm/min. It is also observed that thermal gradient is high enough to melt large volume of material. Hence, a full depth of penetration is observed.

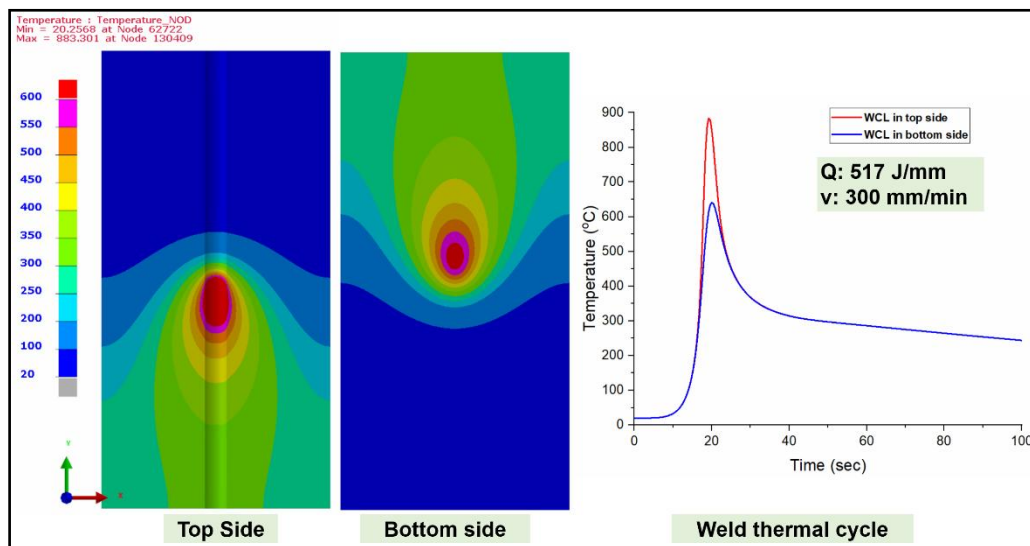


Figure 9. Temperature distribution on the surface for the heat input of 517 J/mm

3.2 Weld bead characterization

The melting temperature of the Aluminum Alloy, AA6061 is 615°C. Hence, the temperature contours are obtained for different combinations of heat input by setting the range of temperature above melting point in the molten pool. Figure 10 shows weld bead profile predicted from finite element simulation and experimental work of MIG welding

for welding current of 160 A and welding speed of 380 mm/min. It emphasizes that the formation of melted material in the FZ is imperative as the surface temperature of the heat source rises beyond 615 °C. The surface area that attains a temperature of above 615 °C gets melted leading to the formation of molten pool.

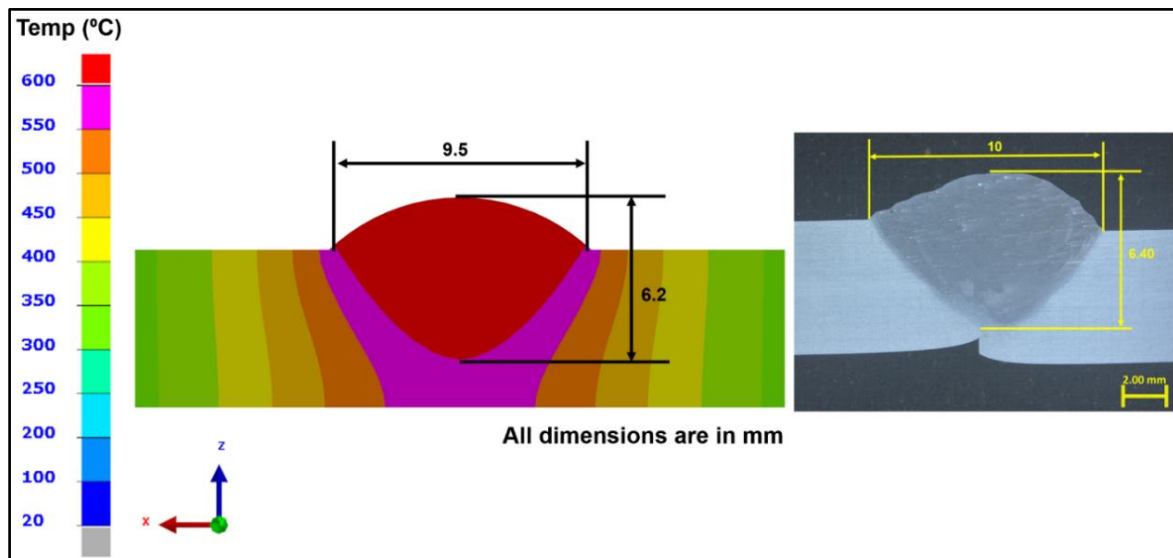


Figure 10. Simulated and experimental weld bead profile

The macrostructure of the experimental weld bead profiles obtained from different welding parameters defined in table 2 and correspondingly compared to simulated weld profiles as shown in figure 11. It is perceived from figure that the weld bead geometry is in good agreement with simulated weld bead profile.

The full depth of penetration is achieved at the highest heat input of 517 J/mm and similarly, the lowest penetration is observed in the lowest heat input of 412 J/mm. It shows that increase in the fusion zone size with increase in heat input which depicts the higher value of heat density applied to the plate surface.

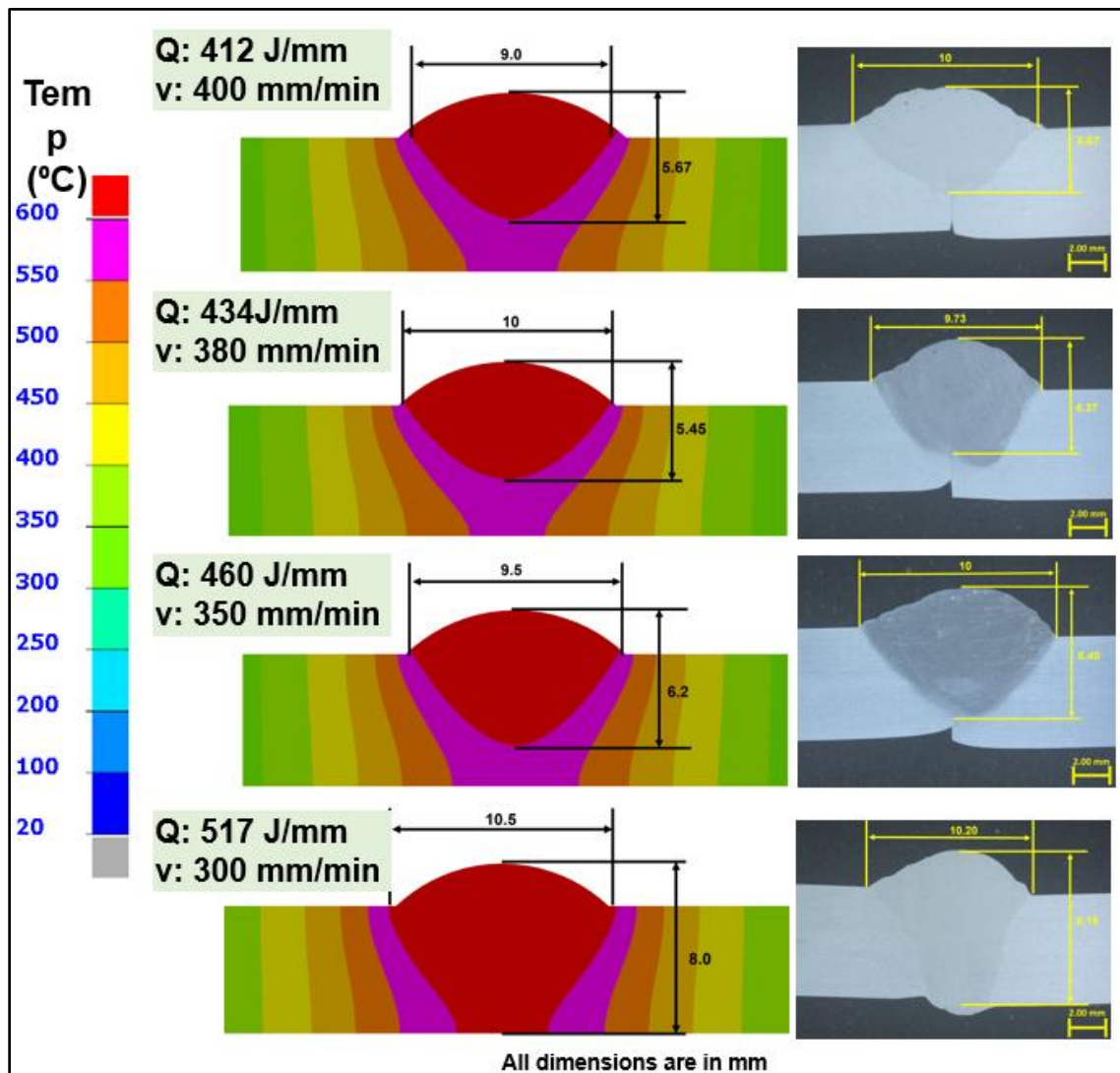


Figure 11. Comparison of simulated weld bead profile with experimental findings

The comparison between the simulated and actual weld bead dimensions gives 90% accuracy of all trails 1 to 4 respectively. Thus the developed heat source model is capable of determining the temperature distribution and weld bead characteristics, which will be capable of optimizing the welding parameters with reduced weld trials.

IV. CONCLUSION

Based on the investigations, the following conclusions are made:

1. Numerical simulation is carried out successfully to predict the weld bead profile and transient thermal distribution during MIG welding of AA6061 alloy.
2. The modelled Double Ellipsoidal Heat Source Model (DEHSM) predicts the temperature distribution of the welded plate, and the simulated

results have good agreement with the experimental findings.

3. The developed heat source model displays better predictability to optimize the process parameters for obtaining the required weld bead geometry such as weld penetration with minimal weld trials.

REFERENCES

- [1]. Tsao L C, Tsai T C, Wu C S, Chuang T H, Brazeability of the 6061-T6 aluminum alloy with Al-Si-20Cu-based filler metals, *Journal of Materials Engineering and Performance*, 2001, 10: 705-709.
- [2]. Hikhale S R, Kolhe K P, Kumar P, Prediction of mechanical properties of Al alloy 6061-T6 by using GMAW. *International Journal of Current Engineering and Technology*, 2016, 5: 300-306.

- [3]. Jogi Bhagwan F, Awale A S, Nirantar S R, Bhusare H S, Metal inert gas (MIG) welding process optimization using teaching-learning based optimization (TLBO) algorithm, *Materials Today: Proceedings*, 2018, 5: 7086–7095
- [4]. Lindgren, L. E, Finite Element Modeling and Simulation of Welding. Part 1: Increased Complexity. *J. Therm. Stresses* 2001, 24, 141–192.
- [5]. Yadaiah N, Bag S, Effect of heat source parameters in thermal and mechanical analysis of linear GTA welding process. *ISIJ Inter* 2012; 52:2069e75.
- [6]. Fachinotti VD, Cardona A, Semi- analytical solution of the thermal field induced by a moving double-ellipsoidal welding heat source in a semi-finite body. In: *The Mech. Comput. Carlos Zuppa*; 2008. p. 1519e30. 10-13 November, San Luis, Argentina.
- [7]. M. Behulova, D. Svrcek, Analysis of the influence of parameters of Goldak model on the computed temperature distribution in a weld, *Slovak university of technology in Bratislava, Paulinska 16, 917 24 Trnava, Slovak Republic*.
- [8]. Francis J D, *Welding simulations of aluminum alloy joints by finite element analysis. Virginia Tech*, 2001.
- [9]. Bradac J, Calibration of heat source model in numerical simulations of fusion welding, *Machines, Technologies, Materials*, 2013, 11: 9–12.
- [10]. Ismail M I S, Afieq W M, Thermal analysis on a weld joint of aluminium alloy in gas metal arc welding, *Advances in Production Engineering & Management*, 2016, 11: 29–37.
- [11]. Vargas Javier A, Torres Jaime E, Pacheco Jovanny A, Hernandez Roque J, Analysis of heat input effect on the mechanical properties of Al-6061-T6 alloy weld joints, *Materials & Design*, 2013, 52: 556–564.
- [12]. Baharnezhad S, Golhin A P, In-situ measurement and finite element simulation of thermo-mechanical properties of AA 6063 aluminum alloy for MIG weldment, *Materials Physics & Mechanics*, 2017, 32: 222–236.
- [13]. ASTM E3, Standard Guide for Preparation of Metallographic Specimens, 2017, p. 11.
- [14]. Anca A, Cardona A, Fachinotti V, Finite element modelling of welded joints. *MecánicaComput.* 2008, 27,1445–1470.
- [15]. Deng D, Murakawa H. Numerical simulation of temperature field and residual stress in multi-pass welds in stainless steel pipe and comparison with experimental measurements. *Comput Mater Sci* 2006;37(3):269e77.
- [16]. Shanmugam N.S, Buvashekar G, Sankaranarayanan K, Ramesh Kumar C, A Transient Finite Element Simulation of the Temperature and Bead Profiles of T-joint Laser Welds. *Mater. Des.* 2010, 31, 4528–4542.
- [17]. Goldak J, Chakravarti A, Bibby M, A new finite element model for welding heat sources, *Metall. Trans*, 1984, B 15, 299–305.
- [18]. Gery D, Long H, Maropoulos P. Effects of welding speed, energy input and heat source distribution on temperature variations in butt joint welding. *J Mater Process Technol* 2005; 167:393e401.
- [19]. Chiocca A, Frendo F, Bertini L, Evaluation of Heat Sources for the Simulation of the Temperature Distribution in Gas Metal Arc Welded Joints. *Metals* 2019, 9, 1142.
- [20]. Ravisankar A, Velaga SK, Rajput G, Venugopal S. Influence of welding speed and power on residual stress during gas tungsten arc welding (GTAW) of thin sections with constant heat input: a study using numerical simulation and experimental validation. *J Manuf Process* 2014; 16:200e11.